Modeling and Analysis of Coupled Flow Through Packed Beds as a Diagnostic Tool for Packed Bed Reactor Health – 17172

Thomas S. Zemanian* and Keith Witwer
AECOM Corporation (USA) (*thomas.zemanian@aecom.com)

ABSTRACT

The US Department of Energy, Office of River Protection, is building the Waste Treatment and Immobilization Plant (WTP) in Richland, Washington, to immobilize the hundreds of millions of liters of radioactive waste stored at the Hanford Site in Washington state. The offgas generated during vitrification of these wastes requires treatment to remove and/or destroy chemical and radioactive hazardous components before release to the atmosphere. In particular, volatile and semivolatile hydrocarbon components are to be catalytically oxidized to carbon dioxide and water, whereas nitrogen oxides (NO_x) are to be catalytically reduced to nitrogen and water. These tasks are accomplished in a series of packed bed reactors. Achieving the requisite Destruction/Removal Efficiency (DRE) for each of the tracked components is highly dependent on the flow characteristics of the offgas through the packed beds. The flow kinetics may be monitored and characterized during the initial warmup of the system. The gases, initially at 76°C (169 °F), (a) flow through one side of a countercurrent heat exchanger to recover heat from the exiting gases (which have already passed through the catalytic beds), (b) are then further heated electrically to approximately 400°C (750°F; the preferred operating temperature of the ThermoCatalytic Oxidizer (TCO)), (c) pass through the TCO where the reduced components of the offgas are oxidized over a supported Pt catalyst bed, (d) are partially cooled to approximately 315°C (600°F) by addition of approximately 25% (by weight) diluted ammonia/air mixture, (e) pass through the Selective Catalytic Reducer (SCR) where the NO_x components are converted to N_2 and H_2O over a supported V_2O_5/TiO_2 catalyst bed, and (f) exit through the hot side of the countercurrent heat exchanger. The electrical heater is not powerful enough to raise the temperature of the offgas to the desired 400 °C without the contribution of the heat recovered in the heat exchanger. Moreover, the thermal mass of the beds and housings of the TCO and SCR require a significant input of thermal energy to reach the desired operating temperatures; the better part of a day is required to bring the unit from ambient temperatures to operating temperatures. Therefore, the temperature of the stream during the initial warmup of the system at each point in the system is dependent upon the thermal mass, flow dispersion, and permeability of the components, quantified as characteristic/representative volumes and residence times. By monitoring the temperature of the offgas as it enters and exits each portion of the system during this warmup period one may model the system as a series of small Continuously Stirred Tank Reactors (CSTR)s (referred to as "CSTRlets") to explain the flow kinetics through the catalyst beds. These component CSTRlets are adjustable in size and number, that one may model the flow profile of the gases through the catalyst beds. For example, a single large CSTR will present an effluent temperature profile with a simple exponential decay shape. Concatenating more

CSTRlets generate more complex sigmoidal responses. Concatenating one CSTRlet significantly larger than the others in the train also alters the shape of the effluent temperature profile, in a fashion not replicable by a train of equal-sized CSTRlets. The ultimate goal is to accurately emulate the entire system as a representative CSTRlet train. Once accomplished, this characterization may be used in subsequent warmups (following shutdown for catalyst maintenance, for example) or by an intentional step change in inlet offgas temperature to detect/diagnose anomalies in flow through the beds (e.g., channeling or partial blockage.) This work presents development of this model through analytical, calculational, and empirical means.

- The analytic model is accomplished by Laplace transform analysis of each component to recover component process transfer functions.
- The calculational portion is performed via brute force finite element calculation.
- Fitting empirical data from the warmup of the TCO skid allows one to select the hypothetical CSTRlet trains which best fit the TCO and SCR beds for the analytical and finite element calculations.

The first portion of this paper presents the development of the analytical (Laplace space) model of the coupled system. Estimated values for the initial temperature, mass, specific heat, electrical heat, and relative quantities of the offgas, catalyst beds, stainless steel housings, and ammonia dilution stream are used to generate expected temperature profiles at several selected junctures of the system. The number and size of the component hypothetical CSTRlets are calculated from the analytical model and are used to predict temperature profiles at the exit of the system and at intermediate junctions between system components (where thermocouples are present in the actual unit.) The finite element calculations employ a series of CSTRlet volumes to produce a similar suite of temperature profiles, for comparison with the analytical model results. Finally, empirical data from the Factory Acceptance Test system warmup are used to select and compare the results from each modeling strategy to select the CSTRlet train(s) which best model the behavior of the actual system. This work presents a novel method of system component characterization, of value to the WTP plant and similar vitrification facilities as well as chemical process industries unrelated to waste management.

INTRODUCTION

The entire catalytic system (referred to as the "TCO skid") is comprised of more than simply the two catalytic beds, and is represented by the schematic diagram of Figure 1, below.

The gases, initially at 76°C (169°F), enter through the cold side of the heat exchanger, over the electrical coils of the heater, pass through the TCO, the ammonia injection manifold, and the Selective Catalytic Reducer (SCR), and exit through the hot side of the countercurrent heat exchanger. The temperature of the stream is raised in the cold side of the heat exchanger and as it passes through the heater, TCO, and SCR. It is lowered in both the ammonia injection manifold (by

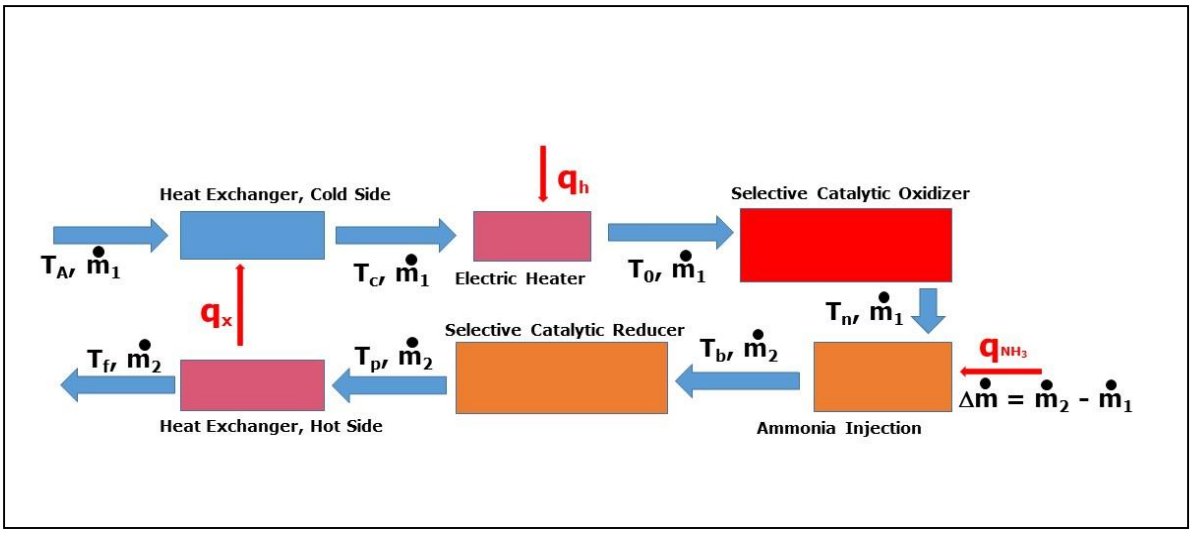

Figure 1: Offgas Catalytic Oxidizer/Reducer Skid

the addition of the cold dilution stream; effectively a removal of specific internal energy represented in figure 1 as q_{NH_3}) and as it passes through the hot side of the heat exchanger. During warmup, however, there are no oxidizable or reducible species present in the stream to generate reaction heat in either the TCO or the SCR. Therefore, the temperature of the stream is actually lowered in these units during warmup, due to the thermal mass of the components. Likewise, the thermal masses of the heat exchanger, electrical heater, and injection manifold cause intrinsic cooling of the stream as it passes through these components as well. Those thermal masses, however, may be subsumed in the CSTRlet trains of the TCO and the SCR.

Moreover, during warmup the ammonia injection is inactive, and hence the entire skid may be modeled as a single CSTRlet train with heat addition in the electrical heater (represented by q_h) and thermal coupling (represented by q_x) in the heat exchanger.

DESCRIPTION

As noted above, the response of the TCO to changes in inlet offgas conditions (temperature, concentrations, etc.) is to be modeled as a response in a set of continuously stirred tank reactors (CSTRs) in series with no chemical reaction[1]. This is a straightforward application of classical Residence Time Distribution theory, applied to a specific case for diagnostic purposes. We begin the analysis by considering a permeable (e.g., packed) bed. By dividing the thermal mass (actual mass times specific heat) of the TCO catalyst and housing into serial components,

[1] This residence time analysis is aimed at the temperature response throughout the TCO at heatup and shutdown. The chemical reaction dynamics through the catalyst beds are not addressed in this paper, as the kinetic behavior of the coupled system is to be modeled only during warmup, before combustible or reducible components are present in the offgas.

the warmup time and overall response to a step function change at the inlet may be represented as a kinetic response partway between a single CSTR and an idealized plug flow reactor (PFR.) An ideal PFR is theoretically equivalent to a series of an infinite number of differentially small CSTRs.

This model is useful for more than merely predicting warmup and cooldown times. It can also serve as a diagnostic tool to assess the health of the flowpath through the TCO. Since heating the TCO itself (comprised of the catalyst beds and the steel of the various components) is accomplished by running heated gas through the TCO, the time for the effluent to reach temperature is indicative of the flow state through the catalyst bed. In other words, should there be a crack or anomaly which allows the offgas to bypass some portion of the catalyst bed, that portion will behave as a conduit rather than an individual (or sequence of) CSTRs and therefore the overall thermal response upon heating will be more CSTR-like than PFR-like, and will be an indicator of an off-normal state.

Porous Bed Response as a Convolution of Series Elements:

The response of a single element (CSTR of mass M [kg]; element "n" is shown as the center element in Figure 2, below) is represented as the ratio of the outlet variable (in this case, temperature) to that at the inlet[2]. Gas flows through the element at flowrate $\dot{m}$ [kg/s]:

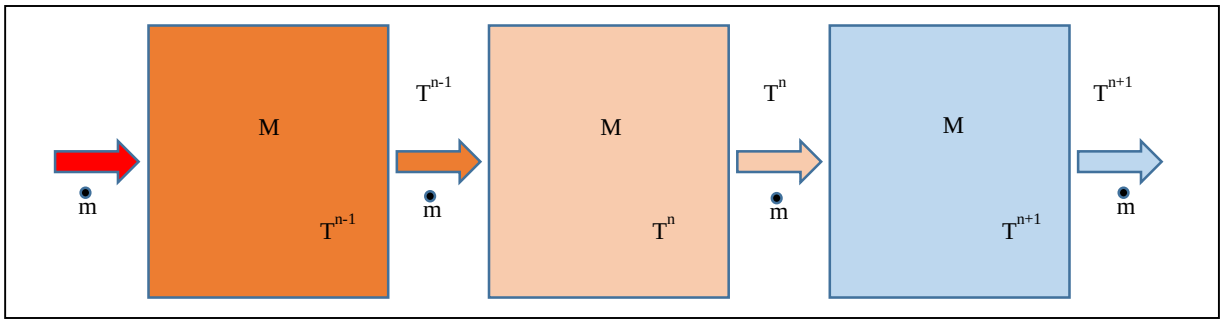

Figure 2: Discretization of a Permeable Bed

The relevant variables and material properties are presented in Table I:

[2]. In this section, "n" is used as an index for a particular CSTRlet in a CSTRlet train. Later the subscript "n" will be used to indicate the stream conditions at the exit of the TCO, as shown in Figure 1. Assuming the TCO model consists of n CSTRlets, the nomenclature is consistent.

TABLE I: Variables and Properties of a Simple Permeable Bed

Variable/Property	Symbol	Unit
Catalyst, resident gas, and housing agglomerate specific heat	$C_{p,cat}$	kJ/kg·°C
Gas specific heat	$C_{p,gas}$	kJ/kg·°C
Inlet temperature	T_{in}	°C
CSTR temperature (identical to outlet temperature)	T_{out}	°C
Ambient temperature (temperature from which warmup starts and to which cooldown ends.)	T_{amb}	°C
Total agglomerate mass of catalyst, resident gas, and housing	M	kg
Gas mass flowrate	$\dot{m}$	kg/s
Time since startup	t	s

Taking T_{amb} as the reference state, a simple energy balance yields:

$$M \cdot C_{p,cat} \cdot d(T_{out}-T_{amb})/dt = \dot{m} \cdot (T_{in}-T_{amb}) \cdot C_{p,gas} - \dot{m} \cdot (T_{out}-T_{amb}) \cdot C_{p,gas}. \quad \text{(Eq. 1)}$$

Replacing $(T_{out}-T_{amb})$ and $(T_{in}-T_{amb})$ with T^n and T^{n-1}, respectively, and defining γ as

$$\gamma \equiv (\dot{m}/M) \cdot (C_{p,gas}/C_{p,cat}) \qquad [s^{-1}] \quad \text{(Eq. 2)}$$

yields

$$dT^n/dt = \gamma \cdot (T^{n-1}-T^n) = \gamma \cdot T^{n-1} - \gamma \cdot T^n. \quad \text{(Eq. 3)}$$

Note that each T^n has the units of Celsius degrees (rather than degrees Celsius); unless T_{amb} is assumed to be 0°C the T^n values are temperature *differences above ambient*, not thermodynamic temperature values.

This is the general first order inhomogeneous ordinary differential equation that governs the behavior of the outlet temperature (T^n) of the n^{th} element in the model. Note that T_{n-1}, the inlet temperature, is not a constant, but rather is the time-varying temperature of the element just upstream of the CSTR element under consideration.

Similar results may be obtained by concatenating equally sized[3] CSTRlets together. A brute force calculation of the first few elements, assuming a step function input to the first unit[4], yields some insight into the behavior of the CSTR chain:

[3] Equal size is assumed at this stage for simplicity. The analysis may be extended to dissimilarly sized CSTRlet, in a straightforward fashion.
[4] in other words, heat-up from ambient using the incoming gas stream to carry the energy into the TCO

$$T_0 = \text{constant (definition}^5\text{)}; \quad \text{(Eq. 4)}$$

$$T^1 = T_0 \cdot \left(1 - \exp\{-\gamma \cdot t\}\right); \quad \text{(Eq. 5)}$$

$$T^2 = T_0 \cdot \left(1 - \exp\{-\gamma \cdot t\} - \gamma \cdot t \cdot \exp\{-\gamma \cdot t\}\right); \quad \text{(Eq. 6)}$$

$$T^3 = T_0 \cdot \left(1 - \exp\{-\gamma \cdot t\} - \gamma \cdot t \cdot \exp\{-\gamma \cdot t\} - \gamma^2/2 \cdot t^2 \cdot \exp\{-\gamma \cdot t\}\right); \quad \text{(Eq. 7)}$$

$$T^4 = T_0 \cdot \left(1 - \exp\{-\gamma \cdot t\} - \gamma \cdot t \cdot \exp\{-\gamma \cdot t\} - \gamma^2/2 \cdot t^2 \cdot \exp\{-\gamma \cdot t\} - \gamma^3/6 \cdot t^3 \cdot \exp\{-\gamma \cdot t\}\right) \ldots \quad \text{(Eq. 8)}$$

And, in general:

$$T^n = T_0 \cdot \left(1 - \exp\{-\gamma \cdot t\} \cdot \Sigma\left[\, t^i \cdot \gamma^i / i! \,\right]\right) \quad \text{(Eq. 9)}$$

where the sum extends over i = [0, n-1]. A further simplification may be achieved by dividing all temperatures by T_0 to define a dimensionless temperature $\zeta^n \equiv T^n/T_0$. (Again, as the T^n are temperature differences above T_{amb}, one need not express them as absolute or thermodynamic temperatures.) Then,

$$\zeta^n = 1 - \exp\{-\gamma \cdot t\} \cdot \Sigma\left[\, t^i \cdot \gamma^i / i! \,\right]. \quad \text{(Eq. 10)}$$

Shift to Laplace Space:

Taking the Laplace transform of the preceding result yields an interesting result:

$$Z^n \equiv L\{\zeta^n\} = 1/s - \Sigma\left[\, \gamma^i / (s+\gamma)^{i+1} \,\right] = (1/s) \cdot (\gamma/(s+\gamma))^n \quad \text{(Eq. 11)}$$

where Z^n is the Laplace transform of ζ^n.

Recognizing that the Laplace transform of the step function input (a Heaviside function at t=0) is 1/s generates the insight that adding an element (or "cstarlet") involves a convolution of the preceding chain with the function:

$$\eta \equiv \mathcal{L}^{-1}\{\gamma/(s+\gamma)\} = \gamma \cdot \exp\{-\gamma \cdot t\} \quad \text{(Eq. 12)}$$

[5] Defining T_0 to be constant represents the first step in modeling the system. When suitable instrument functions to model the heater and heat exchanger are incorporated, the inlet function will no longer be constant, and the feedback from the effluent to the inlet function makes the model circular. As we shall see, knowledge of the heat exchanger effectiveness allows closed analytic solution of the model even given the time lags associated with the stages and CSTRlet discretization of the catalyst beds.

where η is the inverse Laplace transform of the expression $\gamma/(s+\gamma)$. Interpreting η as the instrument function of a single CSTRlet allows concatenation of arbitrary numbers of CSTRlets, as well as CSTRlets of differing sizes.

These results, along with the Laplace transform of a delta ("spike") input function and the transform of two serial CSTRlets of different sizes constitute a toolbox of transform elements (see Table II, below) which may be multiplied together in desired combinations and then inverse-transformed to generate the expected time-domain behavior of a desired CSTRlet train. Note that the order in which the CSTRlets are strung together does not alter the final aggregate instrument function; the concatenation of CSTRlets of differing sizes is commutative.

TABLE II: Instrument Function Elements and their Laplace Transforms

Time domain symbol	**Function "f(t)"**	**Laplace domain symbol**	**Transform L{f(t)} ≡ F(s)**
H_c Heaviside function	$F(t)=\{0,\ t<c;\ 1,\ t\geq c$	$\mathcal{H}_c$	e^{-cs} special case $\mathcal{H}_0 = 1/s$
η (cstarlet)	$\gamma e^{-\gamma t}$	E	$\gamma/(s+\gamma)$
η^n (n cstarlets)	$\{(-1)^{n-1}/(n-1)!\}\cdot\gamma^n\cdot t^{n-1}\cdot e^{-\gamma t}$	E^n	$\{\gamma/(s+\gamma)\}^n$
ζ^1	$1-e^{-\gamma\cdot t}$	Z^1	$\gamma/(s\cdot(s+\gamma)) = \mathcal{H}_0\cdot E$
ζ^n	$1 - \exp\{-\gamma\cdot t\}\cdot\Sigma[\ t^i\cdot\gamma^i/i!]$	Z^n	$(1/s)\cdot(\gamma/(s+\gamma))^n = \mathcal{H}_0\cdot E^n$
$\zeta_{1\text{-}2}$	$1-(\gamma_2/(\gamma_2-\gamma_1))e^{-\gamma 1t}-(\gamma_1/(\gamma_2-\gamma_1))e^{-\gamma 2t}$	$Z_{1\text{-}2}$	$(1/s)\cdot(\gamma_1/(s+\gamma_1))\cdot(\gamma_2/(s+\gamma_2)) = \mathcal{H}_0\cdot E_1\cdot E_2$
Delta function	$\delta(t-t_0)$	Δ	e^{-st_0}

A note on nomenclature: superscripts generally indicate the number of CSTRlets incorporated in the element, whereas subscripts indicate the size (i.e., relevant γ) of the comprising CSTRlets. Therefore, E_1^n indicates the Laplace transform of a train of n CSTRlets with $\gamma = \gamma_1$.

This chart is intended to be used to develop porous bed models which emulate the behavior of the TCO during heatup and/or cooldown; significant deviations from the historical model(s) indicate the likelihood of flow anomalies, and hence the possibility of channeling or blockage in the catalyst units. The temperature elements at

1. the inlet to the SCO,
2. between the SCO and the NH_3 injection grid,
3. between the NH_3 injection grid and the SCR, and
4. at the SCR outlet

allow four-location fitting of the predicted model to the observed behavior.

Models can be found by choosing a particular ζ^x model from the second column of Table II. Alternatively, one can generate a custom model by multiplying a Laplace transform element for an inlet signal ($\mathcal{H}_0$ or Δ) with selected E transform elements (with varying γ parameters, if desired), and taking the inverse transform to generate a time-domain model.

Full Skid Model:

Armed with the instrument functions of the porous beds, a full model of the skid depicted in Figure 1 may be developed. First, however, note that the warmup behavior proceeds in two phases. The first phase (phase I) operates the electric heater at full capacity ($q_h = q_{h,max}$) until the temperature at the TCO inlet (T_0) reaches 400°C. The catalyst beds and the skid are not yet at full operating temperature at this point, but to continue heating at full power would risk overheating and damaging the lead portions of the TCO catalyst bed. Therefore, once T_0 reaches 400°C the electrical heater is turned down and controlled to hold T_0 at 400°C for the remainder of the warmup period, termed "phase II."

Note also that, due to the addition of diluted ammonia between the TCO and the SCR the mass flow rate increases from $\dot{m}_1$ to $\dot{m}_2$. The offgas specific heat likewise changes from $C_{p,gas,1}$ to $C_{p,gas,2}$. Heat balances may then be struck around each of the stages in Figure 1 to generate a set of simultaneous equations:

- Balance around the heat exchanger cold side:

$$(T_A-T_0)\cdot\dot{m}_1\cdot C_{p,gas,1} + q_x = (T_c-T_0)\cdot\dot{m}_1\cdot C_{p,gas,1} \rightarrow q_x = (T_c-T_A)\cdot\dot{m}_1\cdot C_{p,gas,1} \quad \text{(Eq. 13)}$$

- Balance around the electric heater:

$$(T_c-T_0)\cdot\dot{m}_1\cdot C_{p,gas,1} + q_h = (T_0-T_0)\cdot\dot{m}_1\cdot C_{p,gas,1} \rightarrow T_c = T_0 - q_h/\dot{m}_1\cdot C_{p,gas,1} \quad \text{(Eq. 14)}$$

$$\rightarrow \mathcal{L}_c = \mathcal{L}_0 - (q_h/T_A\cdot\dot{m}_1\cdot C_{p,gas,1})\cdot(1/s) = \mathcal{L}_0 - k_h\cdot(1/s) \quad \text{(Eq. 15)}$$

where $k_h = q_h/T_A\cdot\dot{m}_1\cdot C_{p,gas,1}$ and $\mathcal{L}_i$ indicates the Laplace transform of $\zeta_i \equiv T_i/T_A$.

- Balance around TCO (expressed in Laplace space, as per Table II):

phase I: $\mathcal{L}_n \equiv \mathcal{L}\{\zeta_n\} = \mathcal{L}_0 \cdot E_1^n$ (assuming n CSTRlets in the TCO) and (Eq. 16)

phase II: $\mathcal{L}_n \equiv \mathcal{L}\{\zeta_n\} = (400\ °C/T_A)\cdot\mathcal{H}_0\cdot E_1^n$ (Eq. 17)

where $E_1 = \gamma_1/(s+\gamma_1)$ and $\gamma_1 = (\dot{m}_1/M_1)\cdot(C_{p,gas,1}/C_{p,cat})$[6]

- Balance around the ammonia addition:

$$T_n\cdot\dot{m}_1\cdot C_{p,gas,1} + q_{NH_3} = T_b\cdot\dot{m}_2\cdot C_{p,gas,2} \quad \text{(Eq. 18)}$$

$$\rightarrow \mathcal{L}_b = (\dot{m}_1\cdot C_{p,gas,1}/\dot{m}_2\cdot C_{p,gas,2})\cdot\mathcal{L}_n + (q_{NH_3}/T_A\cdot\dot{m}_2\cdot C_{p,gas,2})\cdot(1/s), \text{ or} \quad \text{(Eq. 19)}$$

$$\mathcal{L}_b = (1/\rho^*)\cdot\mathcal{L}_n + k_{NH_3}\cdot(1/s) \quad \text{(Eq. 20)}$$

where $\rho^* = \dot{m}_2\cdot C_{p,gas,2}/\dot{m}_1\cdot C_{p,gas,1}$ and $k_{NH_3} = q_{NH_3}/T_A\cdot\dot{m}_2\cdot C_{p,gas,2}$

Note that this treatment models the effect of injection of diluted ammonia as (i) an addition of mass as well as a change in aggregate specific heat, which is captured in the change from γ_1 to γ_2 and (ii) a lowering of temperature, represented by k_{NH_3}. This lowering of temperature is an artificial means of including the cooling effect, but is more algebraically tractable. Using typical values for the mass flow rates and specific heats expected in normal operation indicate that $k_{NH_3} \approx 0.9\text{-}1/\rho^*$. In any case, during warmup k_{NH_3} will be set to zero, ρ^* to 1, and γ_2 to γ_1, indicating no ammonia injection.

- Balance around SCR (expressed in Laplace space, as per Table 2):

$$\mathcal{L}_p \equiv \mathcal{L}\{\zeta_p\} = \mathcal{L}_b \cdot E_2^m \quad \text{(assuming m CSTRlets in the SCR)} \quad \text{(Eq. 21)}$$

where $E_2 = \gamma_2/(s+\gamma_2)$ and $\gamma_2 = (\dot{m}_2/M_2)\cdot(C_{p,gas,2}/C_{p,cat})$

- Balance around the heat exchanger hot side:

$$(T_p-T_A)\cdot\dot{m}_2\cdot C_{p,gas,2} - q_X = (T_f-T_A)\cdot\dot{m}_2\cdot C_{p,gas,2} \rightarrow q_X = (T_p-T_f)\cdot\dot{m}_2\cdot C_{p,gas,2} \quad \text{(Eq. 22)}$$

- Combining Eq. 13 and Eq. 22 to eliminate q_X:

$$(T_p-T_f)\cdot\dot{m}_2\cdot C_{p,gas,2} = (T_c-T_A)\cdot\dot{m}_1\cdot C_{p,gas,1} \rightarrow \rho^*\cdot\mathcal{L}_p - \rho^*\cdot\mathcal{L}_f = \mathcal{L}_c - 1/s \quad \text{(Eq. 23)}$$

The relevant simultaneous equations are given in Table III:

[6] Since the TCO and SCR catalysts are supported on the same ceramic substrate (cordierite), we may assume that $C_{p,cat,TCO} = C_{p,cat,SCR}$

TABLE III: Full Skid Simultaneous Equations

Equation	
14	$\mathcal{L}_c = \mathcal{L}_0 - k_h \cdot (1/s)$
16 (phase 1) 17 (phase 2)	$\mathcal{L}_n \equiv \mathcal{L}\{\zeta_n\} = \mathcal{L}_0 \cdot E_1^n$, and $\mathcal{L}_n \equiv \mathcal{L}\{\zeta_n\} = (400\ °C/T_A) \cdot \mathcal{H}_0 \cdot E_1^n$
20	$\mathcal{L}_b = (1/\rho^*) \cdot \mathcal{L}_n + k_{NH3} \cdot (1/s)$
21	$\mathcal{L}_p \equiv \mathcal{L}\{\zeta_p\} = \mathcal{L}_b \cdot E_2^m$
23	$\rho^* \cdot \mathcal{L}_p - \rho^* \cdot \mathcal{L}_f = \mathcal{L}_c - 1/s$

and the relevant variables are $\mathcal{L}_c$, $\mathcal{L}_0$, $\mathcal{L}_n$, $\mathcal{L}_b$, $\mathcal{L}_p$, and $\mathcal{L}_f$. One more equation is needed to couple the front end of the skid to the back end. This is provided by the heat exchanger effectiveness, given from the manufacturer as ε=82.6%:

$$q_X = \varepsilon \cdot \dot{m}_1 \cdot C_{p,gas,1} \cdot (T_p - T_A) = (T_c - T_A) \cdot \dot{m}_1 \cdot C_{p,gas,1}$$
$$\rightarrow T_p = (T_c - T_A) \cdot (1/\varepsilon) + T_A \qquad \text{(Eq. 24)}$$

- And dividing by T_A, transforming, and comparing to Eq. 23:

$$\mathcal{L}_p = (1/\varepsilon) \cdot \mathcal{L}_c + (1 - 1/\varepsilon) \cdot (1/s) = (1/\rho^*) \cdot \mathcal{L}_c - 1/(\rho^* \cdot s) + \mathcal{L}_f \qquad \text{(Eq. 25)}$$

Solving these equations simultaneously and defining $\boldsymbol{\Pi} \equiv E_1^n \cdot E_2^m$ yields Table IV.

The first column in this table presents the transformed instrument functions that describe the temperature at each juncture shown in Figure 1. This is a complete description of the coupled system, but is of limited use. The top half of Table IV presents the analytical results for phase I of the warmup, i.e., before the temperature into the TCO has reached the set value of 400°C. Since this condition is only expected during the warmup of the skid, the terms and specifications representing the ammonia addition are irrelevant in this portion. The results are presented for completeness only.

The second column provides the instrument function transforms at each junction under warmup conditions. Since there is no addition of gas at the ammonia injection during system warmup, $\dot{m}_1 = \dot{m}_1$, $C_{p,gas,1} = C_{p,gas,2}$, $q_{NH3} = 0$, and hence $\rho^* = 1$ and k_{NH3}=0. This significantly simplifies the transformed instrument functions. Nevertheless, the results for Phase I are not immediately tractable, and have not been transformed back to time domain space for this effort. As we shall see later, Phase I data may be fitted to the analytical model in Laplace space (frequency domain).

The third column of Table IV presents the results from the full transform analysis, after taking the inverse transform to recover time domain results. Phase II has its own intrinsic simplifications over the full analysis of Phase I. Specifically, both T_0 and T_A are held constant. Not only does this simplify the instrument function chain, it also decouples the entrance to the TCO skid from the exit stream.

TABLE IV: Full Skid Temperatures Over Time

Phase I			
$\mathcal{L}_i$	**Full Transformed Instrument Function**	**at warmup** (k_{NH3}=0, ρ^*=1, & γ_2= γ_1)	ζ_{i_warmup}
$\mathcal{L}_A$=	1/s	1/s	1
$\mathcal{L}_c$=	$1/s\cdot\left[\frac{(1-\varepsilon+\varepsilon\cdot k_{NH3}\cdot E_2^m+\varepsilon\cdot k_h\cdot\boldsymbol{\Pi}/\rho^*)}{(1-\varepsilon\cdot\boldsymbol{\Pi}/\rho^*)}\right]$	$1/s\cdot\left[\frac{(1-\varepsilon+\varepsilon\cdot k_h\cdot\boldsymbol{\Pi})}{(1-\varepsilon\cdot\boldsymbol{\Pi})}\right]$	
$\mathcal{L}_0$=	$1/s\cdot\left[\frac{1+k_h-\varepsilon+\varepsilon\cdot k_{NH3}\cdot E_2^m}{(1-\varepsilon\cdot\boldsymbol{\Pi}/\rho^*)}\right]$	$1/s\cdot\left[\frac{1+k_h-\varepsilon}{(1-\varepsilon\cdot\boldsymbol{\Pi})}\right]$	
$\mathcal{L}_n$=	$1/s\cdot\left[\frac{(1+k_h-\varepsilon)\cdot E_1^n+\varepsilon\cdot k_{NH3}\cdot\boldsymbol{\Pi})}{(1-\varepsilon\cdot\boldsymbol{\Pi}/\rho^*)}\right]$	$1/s\cdot\left[\frac{(1+k_h-\varepsilon)\cdot E_1^n}{(1-\varepsilon\cdot\boldsymbol{\Pi})}\right]$	
$\mathcal{L}_b$=	$1/s\cdot\left[\frac{(1+k_h-\varepsilon)\cdot E_1^n+\rho^*\cdot k_{NH3})}{(\rho^*-\varepsilon\cdot\boldsymbol{\Pi})}\right]$	$1/s\cdot\left[\frac{(1+k_h-\varepsilon)\cdot E_1^n}{(1-\varepsilon\cdot\boldsymbol{\Pi})}\right]$	
$\mathcal{L}_p$=	$1/s\cdot\left[\frac{(1+k_h-\varepsilon)\cdot\boldsymbol{\Pi}+\rho^*\cdot k_{NH3}\cdot E_2^m)}{(\rho^*-\varepsilon\cdot\boldsymbol{\Pi})}\right]$	$1/s\cdot\left[\frac{(1+k_h-\varepsilon)\cdot\boldsymbol{\Pi}}{(1-\varepsilon\cdot\boldsymbol{\Pi})}\right]$	
$\mathcal{L}_f$=	$1/s\cdot\left[\frac{\left[\left(1-\varepsilon/\rho^*-\varepsilon+k_h\cdot(1-\varepsilon/\rho^*)\right)\cdot\boldsymbol{\Pi}+(\rho^*-\varepsilon)\cdot k_{NH3}\cdot E_2^m+\varepsilon\right]}{(\rho^*-\varepsilon\cdot\boldsymbol{\Pi})}\right]$	$1/s\cdot\left[\frac{(1-\varepsilon+k_h\cdot(1-\varepsilon)\cdot\boldsymbol{\Pi})}{(1-\varepsilon\cdot\boldsymbol{\Pi})}\right]$	
Phase II			
$\mathcal{L}_A$=	1/s	1/s	1
$\mathcal{L}_c$=	$1/s\cdot[(\varepsilon/\rho^*)\cdot(T_o/T_A)\cdot\boldsymbol{\Pi}+\varepsilon\cdot k_{NH3}\cdot E_2^m+1-\varepsilon]$	$1/s\cdot[\varepsilon\cdot(T_o/T_A)\cdot\boldsymbol{\Pi}+1-\varepsilon]$	$\varepsilon\cdot(T_o/T_A)\cdot\zeta^{n+m}+(1-\varepsilon)\cdot\mathcal{H}_0$
$\mathcal{L}_0$=	$1/s\cdot(T_o/T_A)$	$1/s\cdot(T_o/T_A)$	T_o/T_A
$\mathcal{L}_n$=	$1/s\cdot(T_o/T_A)\cdot E_1^n$	$1/s\cdot(T_o/T_A)\cdot E_1^n$	$(T_o/T_A)\cdot\zeta^n_1$
$\mathcal{L}_b$=	$1/s\cdot\left[(1/\rho^*)\cdot(T_o/T_A)\cdot E_1^n+k_{NH3}\right]$	$1/s\cdot(T_o/T_A)\cdot E_1^n$	$(T_o/T_A)\cdot\zeta^n_1$
$\mathcal{L}_p$=	$1/s\cdot\left[(1/\rho^*)\cdot(T_o/T_A)\cdot\boldsymbol{\Pi}+k_{NH3}\cdot E_2^m\right]$	$1/s\cdot(T_o/T_A)\cdot\boldsymbol{\Pi}$	$(T_o/T_A)\cdot\zeta^{n+m}$
$\mathcal{L}_f$=	$1/s\cdot(1/\rho^*)\cdot\left[(1-\varepsilon/\rho^*)\cdot(T_o/T_A)\cdot\boldsymbol{\Pi}+k_{NH3}(\rho^*-\varepsilon)\cdot E_2^m-\varepsilon\right]$	$1/s\cdot\left[(1-\varepsilon)\cdot(T_o/T_A)\cdot\boldsymbol{\Pi}-\varepsilon\right]$	$(1-\varepsilon)\cdot(T_o/T_A)\cdot\zeta^{n+m}-\varepsilon\cdot\mathcal{H}_0$

Note that neither $\mathcal{L}_0$ nor $\mathcal{L}_n$ contain terms in k_{NH3} in Phase II, whereas in Phase I they both do. The coupling through the heat exchanger has been broken due to the control by the electric heater to hold T_0 constant.

Note also that the entries for $\mathcal{L}_n$ and $\mathcal{L}_b$ are identical in the second and third columns of both phases. This is not surprising; during warmup the ammonia

injection is inactive and therefore the injection module performs no instrument function. More to the point, however, the third column contains time domain expressions for $\mathcal{L}_b$ and $\mathcal{L}_p$, which reveal ζ^n and ζ^{n+m}, respectively. Comparison of these therefore allow diagnosis of the TCO and SCR catalyst bed flow characteristics.

Phase I behavior can be fitted to the available data in Laplace space, provided the data are collected in regular intervals. The FAT (Factory Acceptance Test) data do not fit this criterion, but by fitting a polynomial to the data a set of evenly spaced data may be generated. Then, the Laplace transform of the FAT data may be calculated as

$$\mathcal{L}_n = \sum_{n=0}^{N} \zeta(n) e^{st} \text{ where N is the number of FAT data,} \quad \text{(Eq. 26)}$$

And the Phase I results may then be fitted in Laplace space to the transformed empirical data.

DISCUSSION

Channeling:

A break or fissure in one of the catalyst beds or modules will reveal itself as a small volume, high throughput CSTRlet in parallel with the healthy CSTRlet. In extreme cases this will manifest as complete bypass of the ruptured CSTR, thereby changing the response of the bed from the normal ζ^n shape to a ζ^{n-1} shape. (The "normal" parameters, n, are to be determined empirically upon first startup.)

However, if the fissure is not catastrophic for the particular CSTRlet, the channeling behavior may then be modeled as a smaller volume CSTRlet in parallel with the healthy CSTRlet, and the transformed instrument function of this damaged CSTRlet may be replaced by $E_{fissure} = \beta \cdot E_{channel} + (1- \beta) \cdot E_1$, where $E_{fissure}$, $E_{channel}$, and E^1 represent the transformed instrument functions of the "damaged", "fully ruptured", and "healthy" CSTRlets, respectively (the first two in parallel to be used to replace the third in the usual construction to model the compromised flow condition.)

Results:

Values for catalyst and housing mass, mass flowrates, heater power, and specific heats were culled from manufacturer datasheets, TCO skid design documents, and expected offgas flowsheets to generate the required values of γ.

The empirical data are values reported from the factory acceptance test. This test was performed in a non-ideal fashion, in that the temperature was measured only around the cold side of the heat exchanger, the electric heater and the selective catalytic oxidizer. Therefore, values are only usable for T_c, T_0, and T_n. The experimentally measured values for ζ_0 and ζ_n are shown on Figure 4 for comparison with theory. From this, it can be seen that the electric heater behaves

much like a single CSTR (which is not surprising given the very low resistance to flow through the heater) whereas the measurement across the TCO indicates a train of approximately two CSTRlets. More complete data incorporating measurements at a greater number of locations during startup will allow a more refined characterization of the skid.

It should be noted that the inlet (feed) temperature is limited by the power available from the heater unit as well as the 454°C upper temperature limit provided by the manufacturer of the TCO catalyst material.

Phase I:

Phase I results are shown in Figure 3 – the relevant FAT data have been fitted to a quadratic and regenerated as a string of thirteen equally spaced (in time) ζ(n). These data have been transformed as described above to render the Phase I FAT data in Laplace space. Although the analytic result does not perfectly fit the data, the general shape is reproduced and fits roughly to a 3 CSTRlet train, provided the value of γ is quadrupled. The inability to reproduce the shape of the data more accurately may be attributed to variations in the heater power during the FAT Phase I; better data (acquired at evenly spaced intervals, with full heater power throughout Phase I, and measured at more locations than simply downstream of the SCO) are planned for the initial startup of the TCO upon commissioning.

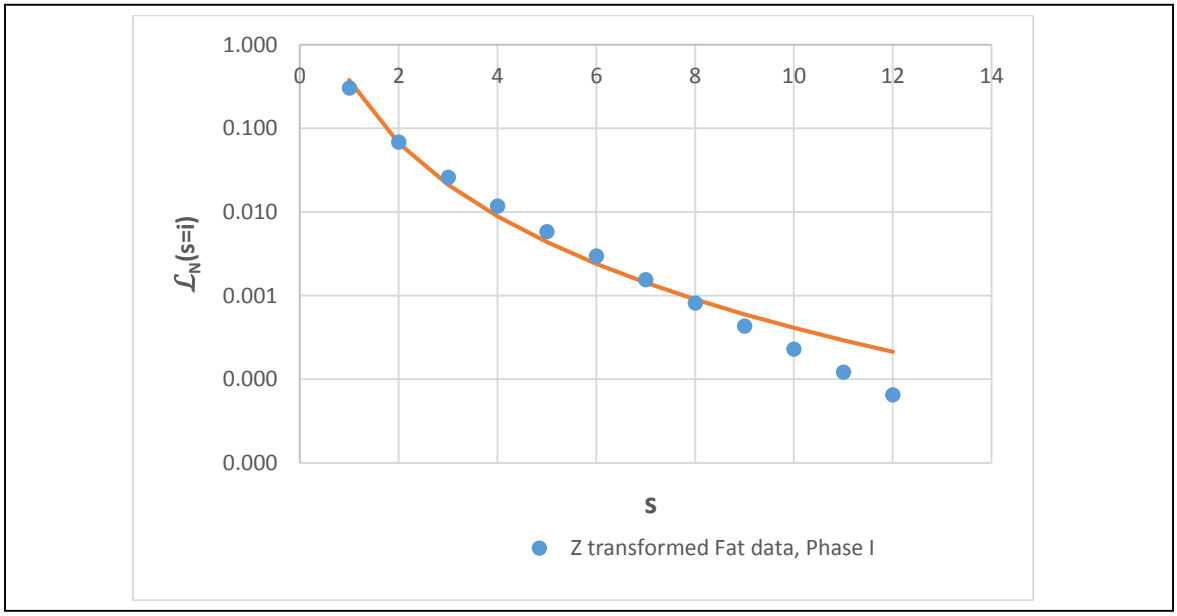

Figure 3: Phase I Analytical Model and Transformed Empirical Results

Phase II:

Calculated values for ζ^{n+m} (Phase II) are shown in Figure 4.

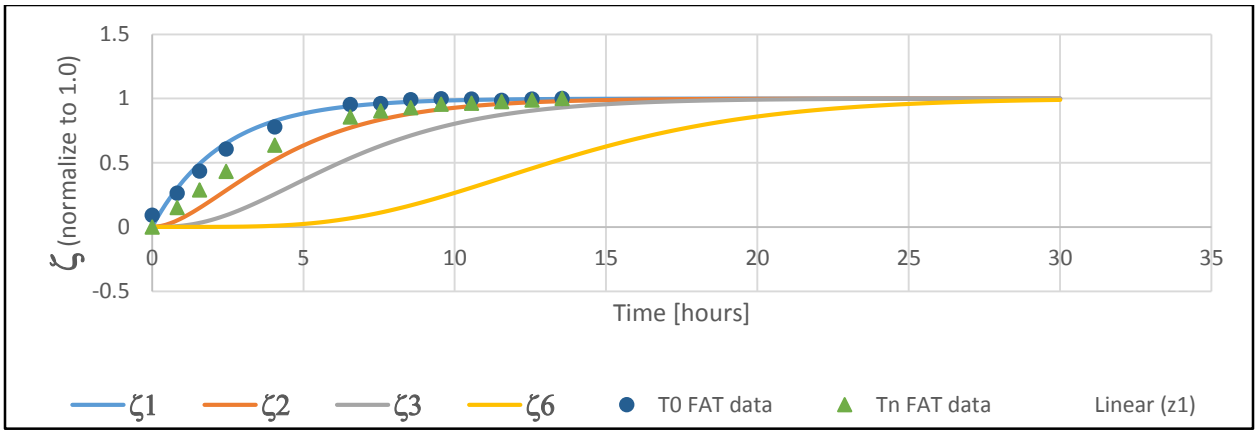

Figure 4: Analytical Calculated and Empirical Results

For both the empirical data and the analytical model the effluent temperature is plotted as a function of time after initial startup (from the inlet temperature) and normalized to the final (target) temperature. Specifically, ζ=0.0 corresponds to an effluent temperature of 71°C (the presumed temperature at the inlet of the heat exchanger) and ζ=1.0 to an effluent temperature of 400°C.

The calculated curves differ in the number of CSTRlets into which the TCO thermal mass has been equally divided. The paucity of the empirical data to which the model is to be compared does not allow for dissimilarly sized CSTRlets, and therefore equally sized division is chosen for simplicity.

Finite Element Model:

Data generated from a finite element model are presented in Figure 5. The finite element generated data yield results similar to those from the analytical model, but cannot be used to model temperatures measured farther downstream than the SCR.

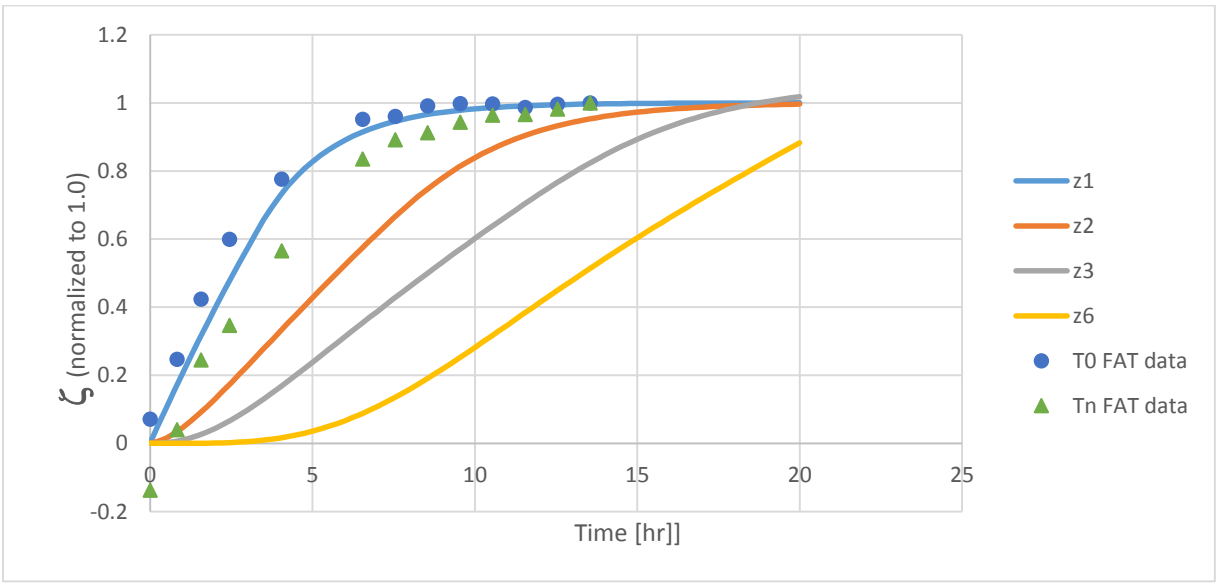

Figure 5: Finite Element Calculated and Empirical Results

Limitations:
There are two noteworthy inherent limitations in the model. The first is that complete energy balance is assumed. In other words, heat loss to the environment is assumed to be negligible. This is most likely not entirely accurate – the insulation cladding the TCO will allow some conductive heat loss, particularly at imperfectly insulated joints. Moreover, piping and ductwork to the TCO will be of a conductive material, and hence introduce a heat sink term into the energy balance.

The second significant shortcoming of the model involves incomplete thermal coupling between the catalyst and housing and the gas stream moving through it. There will almost certainly be transient temperature differences between the hardware and the gas stream as the gas exits the TCO. As a result, some of the heat supplied by the gas stream will be carried out in the exhaust.

A third (but less likely to be significant) limitation of the model involves imperfect mixing across the TCO cross-section. Some regions of the catalyst beds may be warmer than others and thereby result in the thermal analogue of channeling. In other words, cold spots may develop and persist, thereby artificially lowering the thermal mass of the local "CSTRlet."

CONCLUSIONS

The several calculational methods agree roughly in the predicted number of CSTRlets, and provide validation for the method of using warmup time as a diagnostic tool. More careful measurement of warmup times upon commissioning of the offgas system as well as the recording of intermediate temperatures (T_n, T_b, and T_p in particular) during the initial warmup is planned.

REFERENCES

1. Stokes, R.L and E. B. Nauman, "Residence Time Distribution Functions for Stirred Tanks in Series", *Can. J. Chem. Eng.*, 48, 723-725 (1970)

ACKNOWLEDGMENTS

The work described in this paper was performed in support of the U.S. Department of Energy (DOE), Office of River Protection, Hanford Tank Waste Treatment and Immobilization Plant (WTP) Project (contract number DE-AC27-01RV14136), under the URS subcontract to WTP Contractor, Bechtel National, Inc.